ISBN: 978-3-95450-202-8 doi:10.18429/JACoW-HB2018-WEP1WB01

# BEAM DYNAMICS OF THE ESS LINAC

Y. Levinsen*, R. De Prisco, M. Eshraqi, N. Milas, R. Miyamoto, C. Plostinar, A. Ponton
ESS, Lund, Sweden

*Abstract*

The ESS linac will deliver an unprecedented 5 MW of average beam power when completed. Beyond the 90 MeV normal conducting front-end, the acceleration is performed using superconducting structures up to the design energy of 2 GeV. As the ESS will send the beam to a fixed tungsten target, the emittance is not as important a factor as in injectors. However, the losses have to be studied in detail, including not only the average operational loss required to be of less than 1 W/m, but also the accidental losses, losses due to failure and other potentially damaging losses. The commissioning of the ion source and LEBT starts this year and will continue with the RFQ next year. In this contribution we will discuss the beam dynamics aspects and challenges of the ESS linac.

## INTRODUCTION

The ESS accelerator is optimised to produce a maximum neutron flux from the target to the experiments, and so by extent most of the accelerator high level parameters becomes secondary. As an example, the cost optimisation exercise finalised in 2013 resulted in a reduced beam energy on target compensated by an increased beam current to keep the same proton beam power on target (i.e. not affecting the neutron flux) [1].

The nominal design parameters of the ESS are 2 GeV beam on target energy with 62.5 mA proton beam current. The pulse length is 2.86 ms and the machine is pulsed at 14 Hz which equates in a 4 % duty factor. These parameters are realised from acceleration through a normal conducting front end that brings the beam energy to about 90 MeV before a super-conducting main accelerator brings the beam energy to 2 GeV. A contingency space and dogleg brings the beam towards the target where it is painted onto the target using a set of horizontal and vertical rastering dipole magnets, as the target would not be able to take the peak current density for extended period of time without a significant transversal defocusing of the beam.

After the first complete baseline design of the accelerator was ready in 2012 [2], the design has undergone several optimisations to improve performance and/or reliability of the machine, and to cost optimize [1, 3, 4]. In the first major cost optimization, the number of cryomodules was reduced to keep cost down while the beam intensity was increased. In other words, the cost was reduced without decreasing performance, but at an increased risk as higher current is generally harder to obtain reliably. The difficulty of tuning the machine increases due to enhanced space-charge forces, and the margin for the couplers reduces since the more power is consumed by the beam. The contingency space was increased, in order to be able to upgrade to 2.5 GeV beam energy in the future.

An extensive value engineering exercise has been performed across the ESS project, to meet the budget requirements and recover some of the needed contingency funds. That included proposals reducing administrative costs of running the organisation as much as considering descoping options of the machine that will be easy to recover with minimal cost increase once sufficient funds becomes available. Currently the main implication for the accelerator complex is that the number of RF sources for the superconducting linac will be reduced, meaning that the initial beam power on target is reduced from 5 MW to 3 MW [5].

## NORMAL CONDUCTING FRONT END

The beam is generated in a 75 keV microwave discharge ion source [6], which produces a 6 ms beam pulse at 14 Hz with around 90 mA of total current of which around 80 mA are protons. The source is required to deliver the beam pulse with a maximum current fluctuation of 3.5 % at flat top. This type of source is proven to have a very high reliability close to 100 %, and long mean time between failures. It takes around 2 ms for the beam extracted out of the source to plateau, so to get a flat beam pulse we chop off approximately 3 ms of the pulse in the low energy beam transport (LEBT). The beam is focused through two solenoids in the LEBT which also match the beam to the RFQ that then bunches the beam at 352.21 MHz and accelerates it to 3.62 MeV. The last modification of the beam pulse is done by the chopper in the medium energy beam transport (MEBT), that clean the 20 µs of the head of the pulse. This corresponds approximately to the expected transient of the space-charge compensation in the LEBT [7]. The MEBT chopper has a faster rise/fall time of around 10 ns. The overall layout of the ESS linac is shown in Fig. 1. Figure 2 shows a schematic overview of the pulse modifications.

The RFQ is a four-vane type, consisting of 5 sections and a total length of 4.5 m and a minimum aperture of 3 mm radius. The RFQ runs with a Kilpatrik of 1.9 at 352.21 MHz. A relatively long bunching section allows for a high capture and transmission of the matched beam from the LEBT, which is expected to be above 97% [8]. 60 tuners, 2 couplers with two ports each, and 22 pick-ups should provide the needed flexibility to realise an accurate resonant RF through the section.

Both the LEBT and the MEBT contains an extensive set of beam diagnostics to characterise the beam as well as magnetic elements to match the beam transversally to the downstream sections. The MEBT also contains three buncher cavities to focus the beam longitudinally. The main

* yngve.levinsen@esss.se

ISBN: 978-3-95450-202-8 doi:10.18429/JACoW-HB2018-WEP1WB01

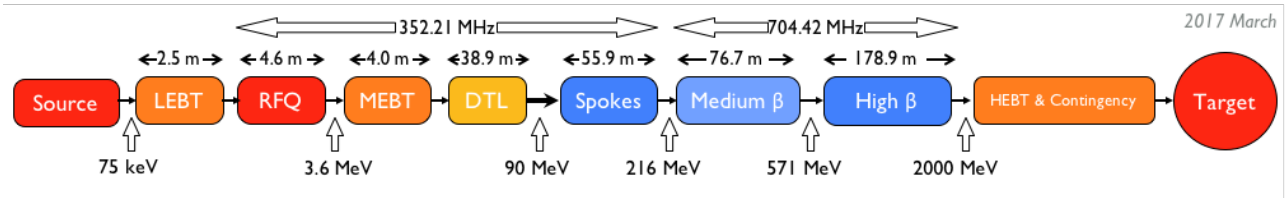


Figure 1: The overall layout of the ESS linac.

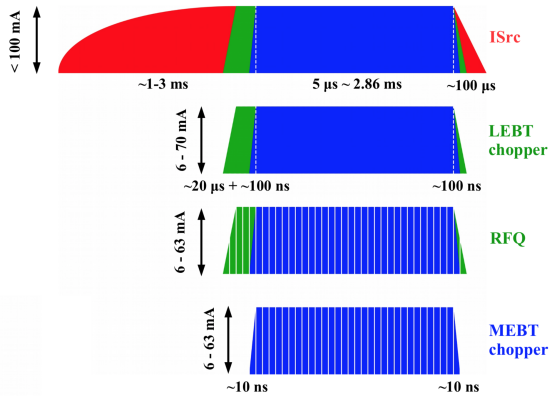


Figure 2: A schematic overview of how the beam pulse changes from 6 ms DC out of the source, to 2.86 ms bunched beam in the ESS front-end. The red part is cleaned by the LEBT chopper, the green cleaned by the MEBT chopper. After the MEBT chopper up to 63 mA beam current remains, with sharp 10 ns pulse edges and a bunching frequency of 352.21 MHz.

chopper is in the LEBT, but has a slower rise time than the fast chopper in the MEBT which purpose is to scrape off the last part of the head and tail of the beam pulse. Details of the LEBT design can be found in [6] and MEBT in [9, 10].

The last section of the normal conducting front end is the DTL, which contains 5 tanks that make up a total length of the section of 38.9 m. The DTL brings the beam energy to 90 MeV [11]. An increase of the beam energy at the entrance of the DTL from 3 MeV in the earlier designs to 3.62 MeV means that the first drift tubes can be longer, which makes them easier to be manufactured and allows for easier installation of quadrupoles. In every second drift tube there is a permanent magnet quadrupole (PMQ), which have a length of 50 mm in tank 1 and 80 mm in tank 2-5.

## SUPERCONDUCTING LINAC

There are three superconducting sections in the ESS linac. There is a low energy differential pumping section (LEDP) that separates the two vacuum levels of the warm front-end from the superconducting linac. First there are spoke cavities running at 352.21 MHz, before a frequency jump to 704.42 MHz where two families of elliptical RF cavities accelerate the beam from around 216 MeV to the final beam on target energy. Between each cryomodule in the superconducting linac there is what is called a linac warm unit (LWU). This unit always consist of a quadrupole pair for focusing the beam transversally, resulting in a FODO lattice.

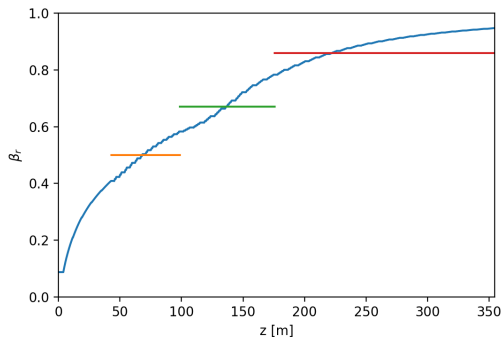


Figure 3: The relativistic β in the ESS linac, with the geometrical β of the three superconducting sections shown as horizontal lines. Spokes in yellow, Mβ in green and Hβ in red.

There is a dual plane trajectory corrector in each LWU, and one BPM. There is also space in the LWU for diagnostics

The spoke cavities bring the beam from 90 MeV to 216 MeV through 13 cryomodules containing a spoke cavity pair each. Spoke cavities were chosen due to their retuning capabilities, and due to their large transversal aperture. The spoke cavities are designed for an optimal relativistic β of 0.5. Details about the Spoke cavity design are described in [12].

Two families of elliptical cavities running at 704.42 MHz follows the spoke cavities. The frequency jump means a sudden drop in the size of the RF bucket, something that will easily be a source of beam losses if not handled carefully. This has been shown in our error studies [13].

The first family is denoted as the medium-β cavities, designed or an optimal relativistic β of 0.67. The second family is denoted the high-β cavities with an optimal relativistic β of 0.86. The relativistic β of the ESS linac is shown in Fig. 3. There are 9 medium-β cryomodules and 21 high-β cryomodules. The elliptical section is designed so that the length of one elliptical period (cryomodule+LWU) is exactly equal at 8.52 m. Each cryomodule holds 4 cavities of 6 cells in the medium-β section and 5 cells in the high-β section. The equal length of LWU's and cryomodules makes everything easily interchangeable should that become useful at some point. The LWU's in the elliptical section of the linac are functionally the same as the spoke LWU's, but offer stronger quadrupole and corrector strength, and larger apertures.

Pulsed quadrupole magnets were considered for the LWU's [14], but they are now abandoned. Using pulsed quadrupoles would greatly reduce the heat load and one

ISBN: 978-3-95450-202-8 doi:10.18429/JACoW-HB2018-WEP1WB01



would be able to operate without water cooling. However the problem with the pulsed magnets is that the eddy currents generated in the conductive beam chamber becomes too large, so the vacuum pipe becomes too hot [15]. Hence the design is now assuming DC magnets again.

## CONTINGENCY AND BEAM TRANSPORT

At the end of the high-β section, the beam has reached the nominal 2 GeV energy. The accelerator has 15 empty slots of same length as medium- and high-β, with the LWU's installed to keep the transversal focusing. This is a contingency space which, if filled with elliptical cavities, will increase the beam on target energy to around 2.5 GeV. After the contingency we have one more LWU before the first dipole of the dogleg. This dipole kicks the beam up at a 4° angle towards the target that is 4.5 m above the beamline of the main accelerator. If this first dipole is turned off, the beam continues straight forward into a defocusing triplet and then the beam hits the tuning beam dump. The dogleg has 12 quadrupoles which maintains a phase advance vertically such that it is an achromatic dogleg allowing longitudinally off-centre particles to follow the same beam trajectory again after the dogleg towards the target.

After the dogleg the beam enters the final section of the accelerator, the accelerator to target (A2T) area. This area consist of 6 quadrupoles that defocuses the beam somewhat and also keep relevant phase advance between critical locations. A rastering system consisting of 4 horizontal and 4 vertical AC dipoles operating at around 30-40 kV paints the beam onto the target in an even Lissajou-pattern [16] and brings down the peak deposited energy density on the target surface. To have this working optimally, one needs control over the phase advance between the second dipole, the action point (centre of rastering system), the cross-over point (location of minimal beam size after last quadrupole) and target surface. Phase advances between these locations should be either 90° or 180° depending on which pair you consider. The most important of those is the action point to cross-over phase advance, which needs to be exactly 90°(+ N×180°).

## STUDIES

One of the main concerns when designing such a high power and perhaps more importantly high intensity linac is the beam losses. In particular when we have a superconducting section it is essential that we keep the operational losses to a minimum and that we have good quantitative and qualitative knowledge of where the losses may occur. Additionally, an rigurous protection system must be in place to detect all possible failures early enough to protect the machine. Which in turn means an extensive evaluation of the possible failures needs to be done beforehand.

There have been several large error studies done on the ESS nominal linac design to verify that the machine is expected to be correctable and that the operational losses are expected to respect the general 1 W/m rule of thumb along the linac [13, 17, 18]. These studies are also used to define the high level requirements of the RF system (amplitude and phase tolerances as seen by the beam), and the larger error studies also provide input to Monte Carlo shower simulations used for example to evaluate locations of beam loss monitors and shielding efficiency.

A perhaps more complex task is to foresee all possible failure modes of a linac. A first step is to look at the effect of blinding out single components (ie single complete failures). This was done for the ESS linac and reported in [19]. For some systems such as the superconducting RF cavities we also looked at the losses arising when the amplitude was decreasing gradually, which allows one to better understand temporal evolution of the losses when knowledge of how quickly the field decays for a given failure scenario is included.

The field flatness in a drift tube linac is strongly dependent on the manufacturing errors, and in turn this affects the stabilization system. The sensitivity of the ESS drift tubes field to the manufacturing errors has been studied and tolerances were defined [20].

The MEBT needs to match the beam to the DTL both transversally through the 11 quadrupoles, and longitudinally through three RF bunchers. Additionally it holds diagnostics and room for the fast chopper and corresponding beam dump. Imperfect matching in the MEBT results in losses downstream, primarily in the DTL but can also cause slow halo growth that results in losses further downstream. The chopper can also be a source of losses if the chopping leaks beam downstream of the chopper dump, and some losses from the partially chopped beam during the chopper rise time is expected [21].

Errors during assembling, brazing and machining of the different parts of the RFQ can result in deviations from the theoretical inter-vane voltage. This alters the quadrupolar components and adds dioplar terms. The errors can be compensated to some extent by tuners. The effect of these errors on the beam dynamics was reported in [8, 22]. The effects of the simplified DTL model typically used in simulations were evaluated in [23] by simulating with detailed 3D field maps of the DTL.

The transmission of the beam through the front-end is an important consideration. Not so much because the losses are necessarily problematic - the beam energy is low so a certain fraction of beam losses can occur without damage to the beam pipe. However one needs to be able to capture enough beam to fulfil the nominal beam parameters. The emittance needs to be small enough so that it fits within the acceptance of the downstream linac, but also not so small that the space-charge forces blows up the beam while the beam energy is still low. Further, a lossy beam in the front end typically drags with it a more dominant halo, which in turn causes losses further downstream where they are more problematic. The transmission studies of the LEBT and RFQ was reported in [24, 25], and it is expected that the ESS front-end will be capable of providing a high capture rate in the RFQ and a very good transmission.

ISBN: 978-3-95450-202-8 doi:10.18429/JACoW-HB2018-WEP1WB01

## STATUS AND OUTLOOK

A primary concern of the ESS linac is to maintain the very low beam losses even at nominal 5 MW beam power, and many detailed studies have been undertaken to evaluate this, either directly or indirectly. Sections of the linac have been studied independently and larger integrated studies have been done to understand the sum of the effects at play. The ESS lattice design has reached mature stage, and should be capable of delivering the most powerful neutron beam in the world as promised. Today we are closing in on the very first commissioning stages of the accelerator complex [26], and exciting times lie ahead.

## REFERENCES


[1] M. Eshraqi, H. Danared, and D. McGinnis, "Design options of the ESS LINAC," in *Proc. IPAC'13*, Shanghai, China, 2013, paper THPWO072.

[2] "ESS technical design report," Tech. Rep. ESS-doc-274-v15, 2013.

[3] M. Eshraqi *et al.*, "The ESS linac," in *Proc. IPAC'14,* Dresden, Germany, 2014, paper THPME043. DOI: 10.18429/JACoW-IPAC2014-THPME043.

[4] E. Bargallo *et al.*, "Value engineering of an accelerator design during construction," in *Proc. IPAC'17*, Copenhagen, Denmark, 2017. DOI: 10.18429/JACoW-IPAC2017-MOPIK040.

[5] C. Plostinar, M. Eshraqi, R. Miyamoto, and M. Munoz, "Beam Commissioning Planning Updates for the ESS Linac," in *Proc. IPAC'17*, Copenhagen, Denmark, 2017. DOI: 10.18429/JACoW-IPAC2017-TUPVA131.

[6] L. Neri *et al.*, "Improved design of proton source and low energy beam transport line for European Spallation Source," *Review of Scientific Instruments*, vol. 85, no. 2, 02A723, Feb. 2014, ISSN: 0034-6748, 1089-7623. DOI: 10.1063/1.4832135.

[7] N. Chauvin, O. Delferrière, R. Duperrier, D. Uriot, R. Gobin, and P. A. P. Nghiem, "Source and injector design for intense light ion beams including space charge neutralisation," in *Proc. LINAC'10*, Japan, 2010, paper TH302.

[8] A. Ponton, Y. I. Levinsen, E. Sargsyan, A. C. France, O. Piquet, and B. Pottin, "Voltage Error Studies in the ESS RFQ," in *Proc. IPAC'16,* Busan, South Korea, Jun. 2016, paper THPMB039. DOI: 10.18429/JACoW-IPAC2016-THPMB039.

[9] R. Miyamoto, B. Cheymol, M. Eshraqi, and I. Bustinduy, "Beam Physics Design of the ESS Medium Energy Beam Transport," in *Proc. IPAC'14*, Dresden, Germany, 2014, paper THPME045. DOI: 10.18429/JACoW-IPAC2014-THPME045.

[10] I. Bustinduy, R. Miyamoto, M. Magan, and F. Sordo, "Current Status on ESS Medium Energy Beam Transport," in *Proc. HB'14*, USA, 2014, paper TU01AB04.

[11] R. de Prisco, M. Eshraqi, *et al.*, "ESS DTL Status: Redesign and Optimizations," in *Proc. IPAC'14*, Dresden, Germany, 2014, paper THPME041. DOI: 10.18429/JACoW-IPAC2014-THPME041.

[12] D. Reynet *et al.*, "Design of the ESS Spoke cryomodule," in *Proc. SRF'13*, Paris, France, 2013, paper MOP089.

[13] Y. I. Levinsen, M. Eshraqi, R. Miyamoto, M. Munoz, A. Ponton, and R. De Prisco, "Beam Dynamics Challenges in the ESS Linac," presented at the HB'16, Malmoe, Sweden, 2016. DOI: 10.18429/JACoW-HB2016-TUAM3Y01.

[14] M. Eshraqi *et al.*, "ESS Linac Beam Physics Design Update," in *Proc. IPAC'16,* Busan, South Korea, 2016, paper MOPOY045. DOI: 10.18429/JACoW-IPAC2016-MOPOY045.

[15] R. De Prisco, E. Sargsyan, and M. Ferreira, "Heating of the Q6 vacuum chamber," Jun. 10, 2016.

[16] H. D. Thomsen and S. P. Møller, "A linear beam raster system for the european spallation source?" In *Proc. IPAC'13*, Shanghai, China, 2013, paper MOPEA005.

[17] M. Eshraqi, R. De Prisco, R. Miyamoto, E. Sargsyan, and H. Thomsen, "Statistical Error Studies in the ESS Linac," en, en, JACOW, Geneva, Switzerland, Jul. 2014, pp. 3323–3325, ISBN: 978-3-95450-132-8. DOI: 10.18429/JACoW-IPAC2014-THPME044.

[18] Y. I. Levinsen, "ESS 2015 baseline lattice error study," Tech. Rep. ESS-0049433, Feb. 2016.

[19] M. Eshraqi, R. de Prisco, R. Miyamoto, and Y. I. Levinsen, "Preliminary Study of the Possible Failure Modes of the Components of the ESS Linac," European Spallation Source ERIC, Tech. Rep. ESS/AD/0057, 2015.

[20] R. De Prisco, M. Eshraqi, A. Karlsson, Y. Levinsen, and R. Miyamoto, "Implication of manufacturing errors on the layout of stabilization system and on the field quality in a drift tube linac - rf dtl error study," in *Proc. LINAC'16*, East Lansing, MI, USA, Sep. 2016, pp. 290–293, ISBN: 978-3-95450-169-4. DOI: 10.18429/JACoW-LINAC2016-MOPLR069.

[21] R. Miyamoto *et al.*, "Dynamics of bunches partially chopped with the MEBT chopper in the ESS linac," in *Proc. LINAC'14*, Geneva, Switzerland, 2014, paper MOPP039.

[22] A. Ponton and A. C. France, "Predictability of the beam quality during RFQ voltage tuning," in *Proc. IPAC'17*, Copenhagen, Denmark, 2017. DOI: 10.18429/JACoW-IPAC2017-MOPIK096.

[23] R. De Prisco, M. Eshraqi, A. Karlsson, Y. Levinsen, R. Miyamoto, and E. Sargsyan, "Effect of the Field Maps on the Beam Dynamics of the ESS Drift Tube Linac," in *Proc. IPAC'15*, Richmond, VA, USA, 2015, paper THPF078. DOI: 10.18429/JACoW-IPAC2015-THPF078.

[24] Y. I. Levinsen, M. Eshraqi, L. Celona, and L. Neri, "In-depth analysis and optimization of the european spallation source front end lattice," in *Proc. IPAC'16,* Busan, South Korea, Jun. 2016, paper TUPMR020. DOI: 10.18429/JACoW-IPAC2016-TUPMR020.

[25] O. Midttun, Y. I. Levinsen, R. Miyamoto, and C. Plostinar, "Benchmarking of the ESS LEBT in TraceWin and IBSimu," in *Proc. IPAC'17*, Copenhagen, Denmark, 2017. DOI: 10.18429/JACoW-IPAC2017-THPVA013.

[26] N. Milas *et al.*, "ESS commissioning plans," presented at the HB'18, Daejeon, Korea, Jun. 2018, paper TUA1WD01.